

# Characterization of Microelectrode Array of Dielectrophoretic Microfluidic Device

Nurul Amziah Md Yunus<sup>1\*</sup>, Zurina Zainal Abidin<sup>2</sup> and Izhal Abdul Halin<sup>1</sup>

<sup>1</sup>Department of Electrical and Electronic Engineering and Advanced Material Synthesis and Fabrication Laboratory (AMSF), Faculty of Engineering, Universiti Putra Malaysia, Serdang, Selangor, Malaysia

<sup>2</sup>Department of Chemical and Environmental Engineering, Faculty of Engineering, Universiti Putra Malaysia, Serdang, Selangor, Malaysia

## Abstract

This paper presents the characterization of angled microelectrode array as dielectrophoretic microfluidic device for the continuous flow-through separation of particles. The operation of the device is demonstrated using samples of colloidal latex beads of 1  $\mu\text{m}$  and 2  $\mu\text{m}$  in diameter sizes, achieving 100% particle deflection with operating voltage as low as 10V and frequency as minimum as 1 MHz. This characterization is essential for dielectrophoretic separation to get the specific suggestion for each type of particle behavior via its own deflection throughout the arrays of the angled microelectrode. The paper also exhibits and discusses the detail of the theoretical background of the separation method; the structure of the device and also the result obtained that is achievable by choice of voltage and frequency.

**Keywords:** Dielectrophoresis; Characterization; Separation; Angled microelectrode

## Introduction

Dielectrophoretic separation has been demonstrated by several groups in the area of biology, chemical engineering and any related as a batch and continuous mode of separation [1]. The research on dielectrophoresis is nonstop by many groups as multidisciplinary teams, including those in chemical, biology, mechanical and electronics engineers. Generally these groups will design device in miniaturization scale for microfluidic application.

Some particle separation devices consist of planar microelectrode arrays such as interdigitated, polynomial and castellated microelectrodes embedded in microfluidic channels. They are used to separate particles using individual or a combination of positive and negative dielectrophoresis (voltage and frequency dependent).

## Dielectrophoresis Force and Angled Microelectrode Design

Electrokinetic is defined as the study of fluid or particle motion in electric fields and generally works in direct current, DC and in alternating current, AC. It includes electrophoresis (EP), dielectrophoresis (DEP), electro-osmosis (EO), electrorotation (ROT) and electroorientation [2-4]. These electrokinetic processes are able to manipulate, concentrate, focus and separate different types of particles, bioparticles or biomolecules.

DEP arises from the interaction of a non-uniform electric field and the polarization induced in the particle. When the polarization of the particle is greater than the polarization of the fluid, the particles will move to high electric field strength (positive DEP). Otherwise the particles will move to low electric field strength (negative DEP).

A significant contribution to bio-dielectric theory was made using DEP, TWDEP and ROT, by Pethig et al. [5-14]. in Bangor, Wales, UK. DEP applications have been demonstrated by Fuhr et al. [15-19] and Gimsa et al. [20-23]. in Germany using embedded microelectrodes in microfluidic devices. This is a different method compared to other techniques, for example, separation is achieved by filtration or centrifugation where no electrode activation is needed [24]. Although effective, filtration and centrifugation methods are not suitable for

integrated systems due to the fact that centrifugation requires the sample to be placed at some distance from the center of rotation in order to achieve a high enough centrifugal force. This requires an elaborate setup, thus not practical in integrated systems. On the other hand, filtration requires membranes, which are susceptible to clogging. Moreover, filters are difficult to mass-produce as part of a microfluidic circuit.

The DEP technique was formalized by Pohl, providing an equation for the dielectrophoretic (DEP) force [2,25]. The simplest DEP expression is that when an AC signal is applied to a homogeneous solid dielectric particle of diameter '2a' suspended in a homogeneous dielectric medium. Both dielectrics will polarize and charge is induced at the interface between the particle and the medium. Opposite charge on either side of the particles produces an effective dipole moment on the particle parallel to the field. An AC field is generated by applying potential of single frequency,  $\omega$ . Therefore the time averaged force on the particle is [2,26]:

$$\langle \mathbf{F}_{DEP} \rangle = \frac{1}{2} \text{Re} \left[ \tilde{\mathbf{p}} \cdot (\nabla) \tilde{\mathbf{E}}^* \right] \quad (1)$$

where  $\tilde{\mathbf{E}}^*$  is a complex conjugate of the electrical field and  $\tilde{\mathbf{p}}$  is the dipole moment  $\tilde{\mathbf{p}} = v \tilde{\alpha} \mathbf{E} e^{i\omega t}$  with  $v$  is the volume of spherical particle,  $\tilde{\alpha}$  is the effective polarizability given by  $\tilde{\alpha} = 3\epsilon_m CMf$ ,  $\epsilon_m$  is the permittivity of the medium and  $CMF$  is the Clausius-Mossotti factor (named after the Italian physicist Ottaviano-Fabrizio Mossotti (1791-1863) and the German physicist Rudolf Julius Emanuel Clausius (1822-1888) [27,28].) which describe the frequency dependence of a dielectric particle's polarizability:

**\*Corresponding author:** Nurul Amziah Md Yunus, Department of Electrical and Electronic Engineering and Advanced Material Synthesis and Fabrication Laboratory (AMSF), Faculty of Engineering, Universiti Putra Malaysia, Serdang, Selangor, Malaysia, Tel: 603-89464368; E-mail: [amziah@upm.edu.my](mailto:amziah@upm.edu.my)

**Received:** May 08, 2016; **Accepted:** May 24, 2016; **Published:** May 31, 2016

**Citation:** Yunus NAM, Abidin ZZ, Halin IA (2016) Characterization of Microelectrode Array of Dielectrophoretic Microfluidic Device. J Bioengineer & Biomedical Sci 6: 190. doi:10.4172/2155-9538.1000190

**Copyright:** © 2016 Yunus NAM, et al. This is an open-access article distributed under the terms of the Creative Commons Attribution License, which permits unrestricted use, distribution, and reproduction in any medium, provided the original author and source are credited.

$$CMf = \left[ \frac{\tilde{\epsilon}_p - \tilde{\epsilon}_m}{\tilde{\epsilon}_p + 2\tilde{\epsilon}_m} \right] \quad (2)$$

$\tilde{\epsilon}_p$  and  $\tilde{\epsilon}_m$  are the complex permittivities of the particle and the medium respectively. The complex permittivities are given by equation  $\tilde{\epsilon} = \epsilon - i\frac{\sigma}{\omega}$ , where  $\epsilon$  is the permittivity and  $\sigma$  is the conductivity of the particle or medium [29-31]. After applying vector identities to equation (3) and assuming that the electric field is real, the expression becomes as shown in equation (3).

$$\langle \mathbf{F}_{DEP} \rangle = \frac{1}{4} v \operatorname{Re}[\tilde{\alpha}] \nabla |\mathbf{E}|^2 \quad (3)$$

$|\mathbf{E}|$  is the magnitude of the electric field. DEP force depends on the induced dipole, the field frequency, the spatial configuration of the field (the gradient of the magnitude  $\mathbf{E}$  squared), the real part of the effective polarizability, volume the particle and more importantly dielectric properties of the suspending medium. By substituting the effective polarizability of the sphere, the expression for the time-averaged DEP force of a sphere becomes,

$$\langle \mathbf{F}_{DEP} \rangle = \pi \epsilon_m a^3 \operatorname{Re} \left[ \frac{\tilde{\epsilon}_p - \tilde{\epsilon}_m}{\tilde{\epsilon}_p + 2\tilde{\epsilon}_m} \right] \nabla |\mathbf{E}|^2 \quad (4)$$

$$\langle \mathbf{F}_{DEP} \rangle = \pi \epsilon_m a^3 \operatorname{Re}[CMf] \nabla |\mathbf{E}|^2 \quad (5)$$

The real part of the  $CMf$  as in equation (5) determines the direction of the DEP force. The particle moves towards high electric field strength region when  $\operatorname{Re}[CMf] > 1$  called positive DEP; the particles are repelled from the high field strength region, when  $\operatorname{Re}[CMf] < 1$  called negative DEP. In this paper, we are concern about the design of the new angled microelectrode array and its characterization which will be used in the separation of mixture of particles, organics or inorganics particles in various fields, such as biology, chemistry, material, environment and many more.

## Method

A batch flow method for separating plugs of particles using only negative DEP has commonly been demonstrated, for example in [9]. However, it relies on gravity to achieve separation. If one would like to separate small submicron and nanoparticles, it will not be possible, due to the negligible influence of gravity on colloidal particles. The separation method chosen in this work is a continuous mode of separation, which involves no contamination of the device (no fouling) ensuring longevity of operation. The concept of the batch flow and the continuous flow are illustrated in Figure 1.

## Device

A new structure of device design consists of chronological arrays of interdigitated microelectrode with angle of 60 degree (i.e. called angled microelectrode) is introduced. The microelectrode width and the inter-microelectrode gap both are 20 $\mu$ m were fabricated on upper and lower surfaces of the microfluidic channel. This device uses negative DEP achieved from the voltage and frequency applied to the top and bottom microelectrodes in the microchannel. The negative DEP used is to achieve gradual deflection through the sequential influence of the electrodes in the array as illustrate in Figure 2.

As illustrated in Figure 2, the larger particles are pushed through outlet A while the smaller particles are deflected along the elongated electrodes and exit the channel through outlet B.

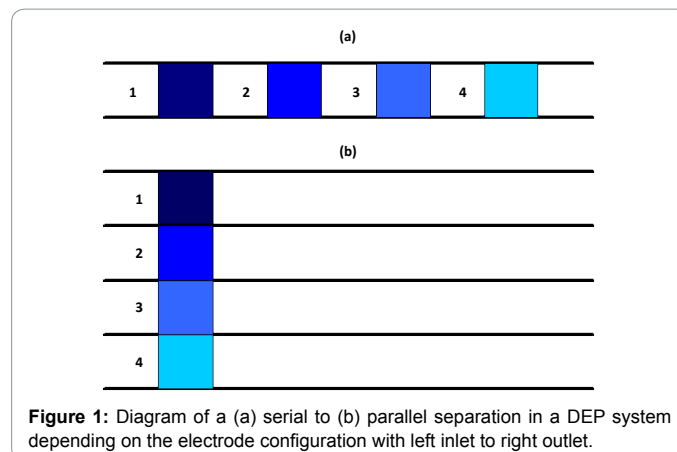


Figure 1: Diagram of a (a) serial to (b) parallel separation in a DEP system depending on the electrode configuration with left inlet to right outlet.

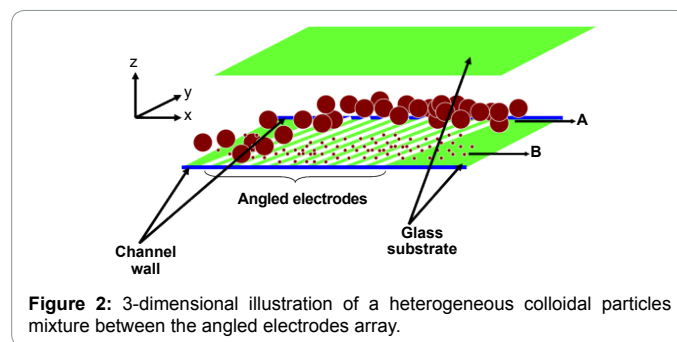


Figure 2: 3-dimensional illustration of a heterogeneous colloidal particles mixture between the angled electrodes array.

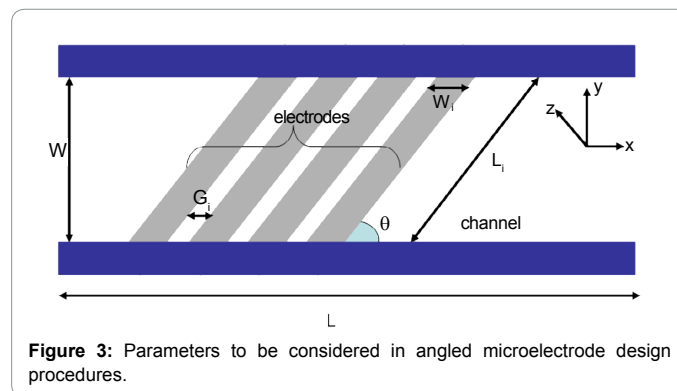


Figure 3: Parameters to be considered in angled microelectrode design procedures.

As the electrode design is further improved over the previous work [32-37] a newer design to increase separation over the angled microelectrode array is found and shown in Figure 3. The requirements and optimizations not only depend on particle size, but also on the device's length,  $L$ , width,  $W$  and height,  $Z$ . Those are important and are based on the following points.

- A single electrode length,  $L_i$  along the channel must be long enough such that a strong DEP force can be generated when multiple electrodes are arranged as an array. The generation of this force is a function of frequency, thus  $L_i$  must be optimized to minimize voltage attenuation at higher frequencies. Here  $L_i=3$  mm.
- The electrode array width,  $W_i$  is optimized to be wide enough for it to have low resistance. The gap between the electrodes,  $G_i$  is designed to be small. This is to induce a strong electric field,

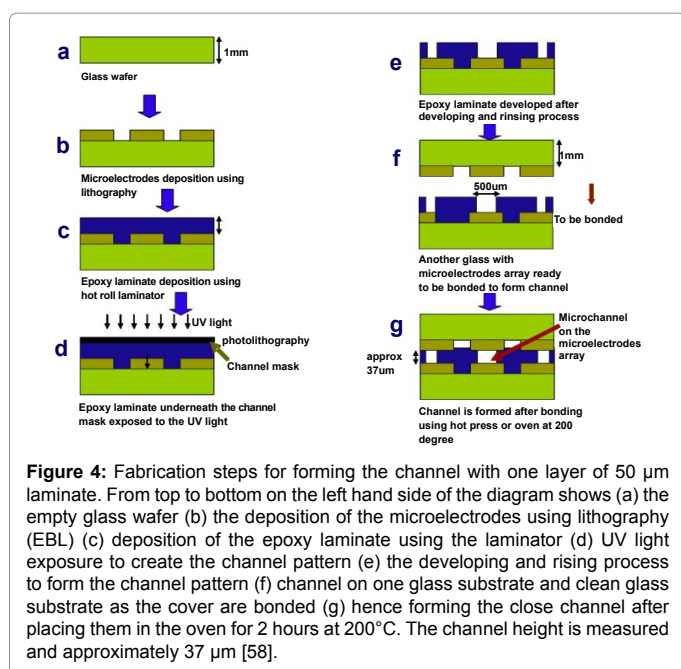
which in turn produces a greater DEP force when voltage is applied to the electrodes. Our  $W_i=20\ \mu\text{m}$  and  $G_i=20\ \mu\text{m}$ .

- The channel length,  $L$ , should be long enough to fit the electrode array.  $L$  heavily depends on the number of electrodes used and is closely related to summation of  $W_i$  and  $G_i$ . It is observed that longer  $L$  values results in higher separation efficiency. In this case  $L=15000\ \mu\text{m}$ .
- The channel width,  $W$ , must be wide enough to accommodate the angled electrode array.
- The channel height,  $z$  is designed to be small in an effort to increase the force on small particles.  $Z=37\ \mu\text{m}$ .
- The angle/inclination of the electrodes,  $\theta$  with the channel wall is optimized in order to increase the distance of particle movement. Our  $\theta=60$  degree.

It is also worth mentioning that a slight placement offset/shifting between the top and bottom electrode arrays results aids in increasing the electric field force and ultimately the DEP force [38]. In this paper, more details on device, setup and results from the particle separation/deflection experiments using the angled microelectrode array will be offered as a continuation from [39]. The tests presented show the suitability of this design to be used in dielectrophoretic separation.

## Device Fabrication

The thickness for the channel in microfluidic device using two layers of dry film resist SY355 of this new design has been decreased to approximately  $37\ \mu\text{m}$  depth, as reported previously [40]. This could increase the electric field strength throughout the microelectrode array and thus the DEP force. Sometimes some researcher will do simulation on the new electrode designed [41]. We also did the simulation and computational fluid dynamics method of DEP force on the microelectrode before the characterization of it is carried out [38]. The step of fabrication is shown in Figure 4.



## Particles

The fluorescent Fluo Spheres, latex spheres particles or latex beads are used in the experiment. They are obtained from Molecular Probes (Eugene, OR). These latex beads are high quality and ultraclean polystyrene microspheres. These latex spheres contain fluorescent dyes and are carboxylate-modified spheres. The spheres have a net negative charge. The advantage of choosing the fluorescent microspheres is that it will help the visualization in the experiment. The other advantages because it is a nontoxic substance and can be used to immobilize antigen that interact with antibody [42,43]. It is also good to be used in microscale channels and parallel sample processing, because of its rapid reactions [44]. As inert particles the benefit include that they may be used in rapid assays with natural populations, require minimal handling of the sample, and can be manipulated in various ways to provide information on different aspects of grazing (e.g. size selection, chemosensory behavior, etc). Latex beads are good as immunologic markers for detecting the interaction of antibody with rare cells. It can be used as a labeling index (beads per bacterial cell) [45,46]. Latex beads can be used as a biomarker [47]. Polystyrene latex beads also can be coated with specific antibodies [45]. These advantages have enabled researcher to identify drug receptors directly from crude cell extracts within less than few hours. Apart from that latex beads can be used for counting [48,49]. and rapid imaging of nanoparticles. Latex beads could be as probes of microorganisms and are used as a measuring aid for microorganism [50,51]. Latex beads are used in real-time particle tracking technology because it can become solid carriers with wide size range; uniformity in size. Latex beads allow higher binding efficiency and less extensive washing. Here, latex beads particles with diameter of  $2\ \mu\text{m}$  and  $1\ \mu\text{m}$  are used as supplied by the manufacturer. These latex beads are the safe used guinea pig for observing the occurrence of the separation in the device system with respect to the actual biological cells later. Two medium conductivities of potassium chloride, KCl where the polystyrene particles are suspended  $14.8\ \text{mS/m}$  and  $1.4\ \text{mS/m}$  are examined. The two mediums are chosen with 10 times difference because it is to observe the different behavioral of these different types of particles in these two medium. Furthermore knowing that the biological cells and molecules, they were easy to be manipulated in the higher medium conductivity thus the test performed would be one best of the expected based on the theory explained [52-54]. and the side effect such as the hydrolysis could be avoided by controlling the frequency [55-58]. Literally, in theory, with reference to equation (4) at higher frequency, the separation in both conductivities is remained approximately the same distance apart. This is because high frequency has immediately eliminated the effect of the conductivity and the force is no longer depending on the conductivity of the particle and medium but it depends on the permittivity of the particle and medium, which in this case, the permittivity of the medium and the particle remain in its fixed values and the force is totally depending on the size of the particle.

## Experimental Works

In the following experiment, the characterization of the device is performed with single particle size deflection. The procedure started by injecting particles at a time into the device. It will be auto-monitored with the program written in Matlab. The program is to execute the particle detection with respect to various voltages and frequencies applied and then analyzed. Figure 5 shows the illustration of the array with captured image at the inlet of measurement A and the captured image at the outlet with measurement B. The result will be the effect of deflection of overall particles over certain voltage and certain frequency applied. Thus the deflection measurement B-A is important.

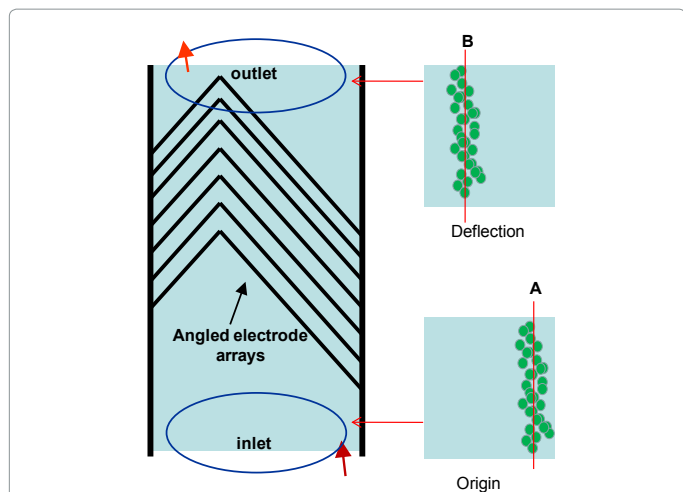


**Figure 5:** Illustration of the top view of the array, with measurement of the deflection of the particle flow through the array from the side wall from point A to point B.

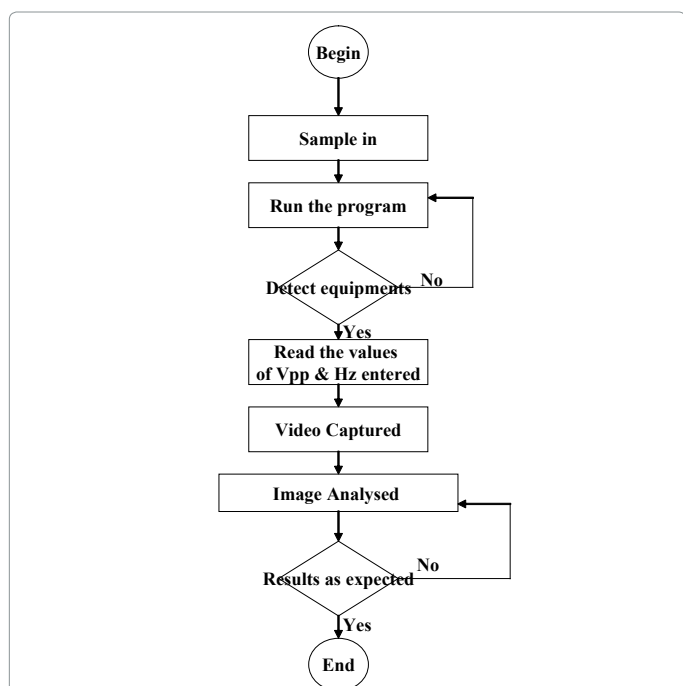


**Figure 6:** The flow chart shows the steps taken for performing the characteristic of the device on single particle deflection.

Figure 6 shows the steps in flow chart environment. It is the procedure to perform the experiment. The data here in the experiment is examined by measuring deflection of particle from the sidewall against frequency at different voltage applied. When these two types of particles are combined together in the channel they can then physically be separated along the arrays, which will be shown in the following section.

### Experimental Results

The characteristic of the device is also obtained by measuring the deflection of one type of particle at a time in the device. The average deflection of 2 μm-sized sphere from the channel wall versus voltage

is plotted and shown in the following Figures. The frequencies applied are below 900 kHz and show a weak deflection of the 2 μm particles in the systems. The voltage applied for this observation is between 0 to 8V. A frequency of 1 MHz is considered as the peak frequency where deflection is at the highest. This is depicted in Figure 7a. For the following frequencies shown in Figure 7b, deflection is constant but as noticed at higher frequencies, a small reduction in deflection is observed due to voltage attenuation. Figure 7 shows that when the voltage is below  $V^2=10$ , no deflection occurs. The particles only flow straight to the output of the arrays. However, when the voltage is increased above the threshold value,  $V^2=10$ , deflection commences and increases in proportions to an increase in voltage.

It is summarized that deflection is limited by voltage attenuation. The frequency range from 1 MHz-4 MHz is the optimum operating frequency range to obtain maximum deflection from the wall for 2 μm-sized particles. It is also observed that the V-shaped electrode geometry causes the tip of the 'V' to act as an end point of deflection.

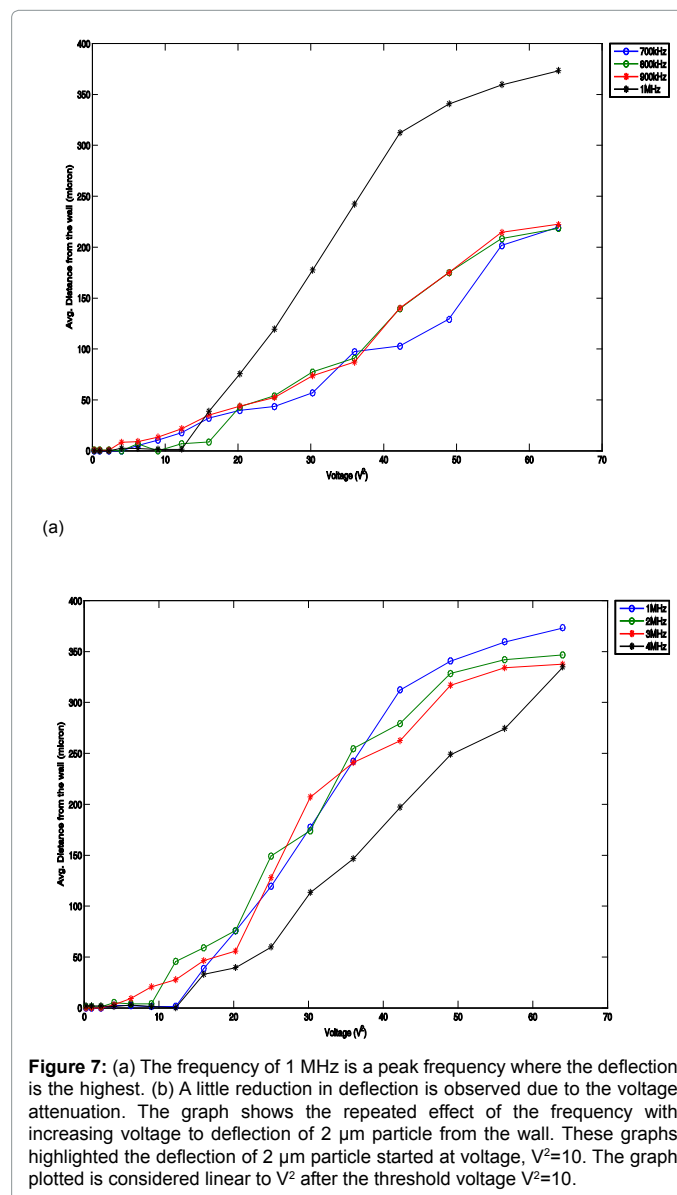


**Figure 7:** (a) The frequency of 1 MHz is a peak frequency where the deflection is the highest. (b) A little reduction in deflection is observed due to the voltage attenuation. The graph shows the repeated effect of the frequency with increasing voltage to deflection of 2 μm particle from the wall. These graphs highlighted the deflection of 2 μm particle started at voltage,  $V^2=10$ . The graph plotted is considered linear to  $V^2$  after the threshold voltage  $V^2=10$ .

Particle deflection adjustments can also be made by adjusting the frequency of operation. At higher frequencies, the deflection is reduced due to voltage attenuation as discussed earlier. This occurrence is shown in Figure 8 where it is observed that particle distance is increased when the frequency is between 700 kHz to 1 MHz.

This is in agreement with increase in DEP force at an optimum frequency range. At low frequencies, the deflection distance does not and at higher frequencies the distance decreases due to attenuation of electrode voltage. This result confirms Clausius Mossotti equation.

Figure 9 shows the deflection of 2  $\mu\text{m}$  sized spheres in a 1.4 mS/m conductive solution as the voltage is increased from 1Vpp to 16Vpp. Practically no deflection is observed below 600 kHz because the 1  $\mu\text{m}$  particle experiences weak positive DEP and nearly strong negative DEP. Deflection starts at a frequency above 700 kHz and when the voltage is increased. Deflection distance remains constant starting from 2.5MHz.

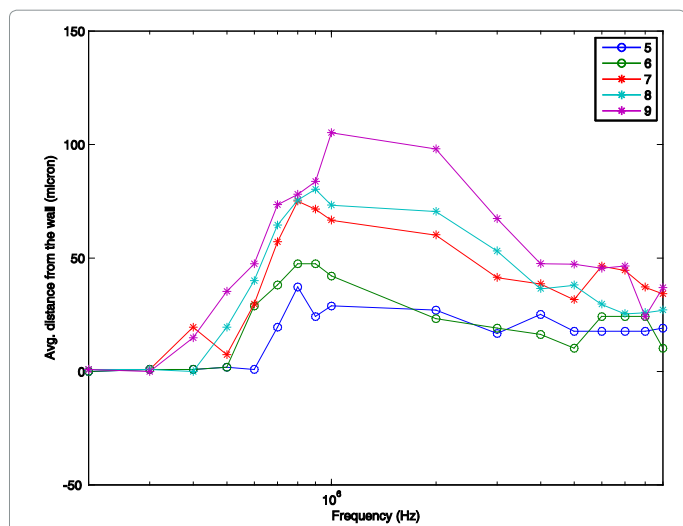


Figure 8: The graph shows the repeated effect of the voltage with increasing frequency to deflection of 2  $\mu\text{m}$  particle from the wall.

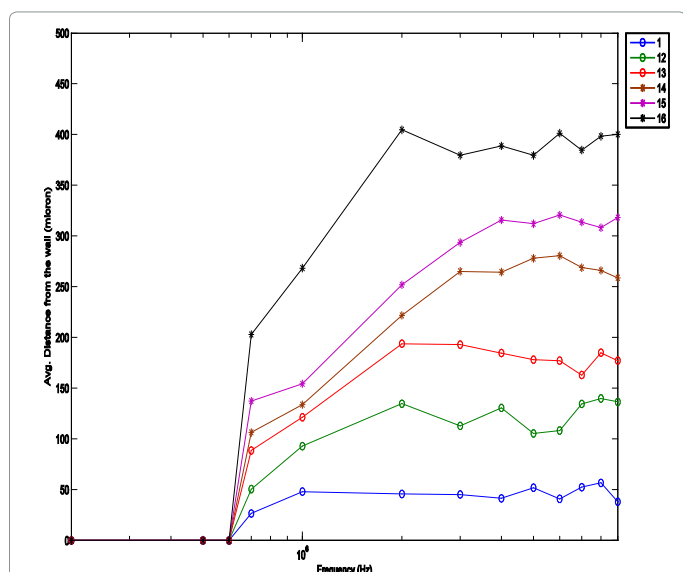


Figure 9: The graph shows the effect of the frequency with increasing voltage to deflection of 2  $\mu\text{m}$  particle from the wall in 1.4 mS/m medium. The voltage is fixed from 1 Vpp up to 16 Vpp.

Figures 10 and 11 show the effect of applied electrode voltage on deflection distance for particles of size 1  $\mu\text{m}$  and 2  $\mu\text{m}$ , respectively. In Figure 10, it can be concluded that by increasing the electrode voltage to 10V (20Vpp), the 1  $\mu\text{m}$ -sized particles is only slightly deflected. However, in Figure 11, the 2  $\mu\text{m}$ -sized particles are deflected significantly and reach the same deflection distance of as it is in a 14.8 mS/m solution [1]. The applied voltage of 10V is the maximum for the 2  $\mu\text{m}$ -sized particles.

Figure 12 shows an estimation of the degree of separation for these two particles combined. The separation does not occur at low frequencies. A threshold frequency of 1MHz is when separation commences. When the medium conductivity is low (100  $\mu\text{M}$  KCl), a lower frequency is enough to trigger separation. At this low concentration, negative DEP is dominant. In a higher conductivity medium, the separation starts to occur in all frequency ranges and

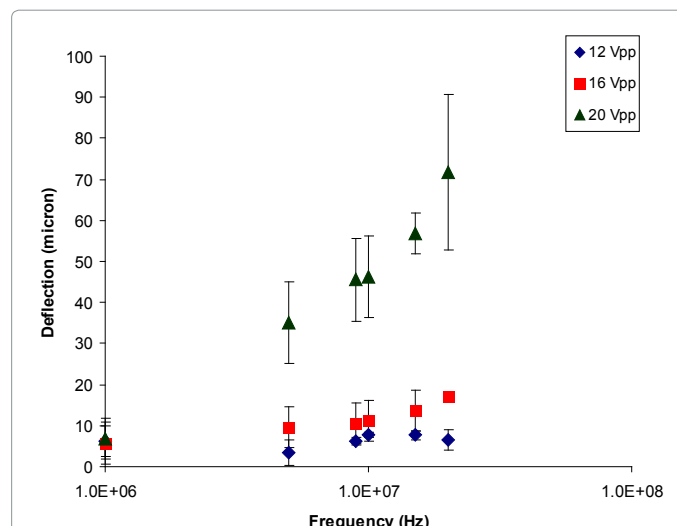


Figure 10: Plots of deflection in 1.4 mS/m KCl at different voltages. The voltage is chosen from 12 Vpp up to 20 Vpp (voltage shown is in Vpp). The graph shows deflection of 1  $\mu\text{m}$  particle from the wall in 1.4 mS/m medium.

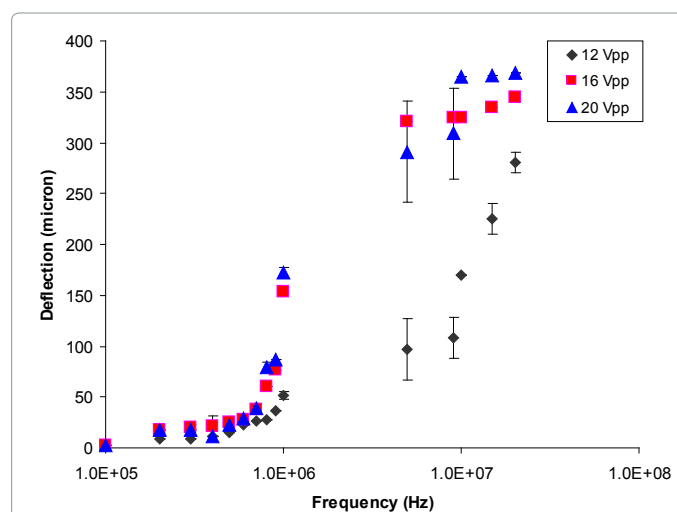
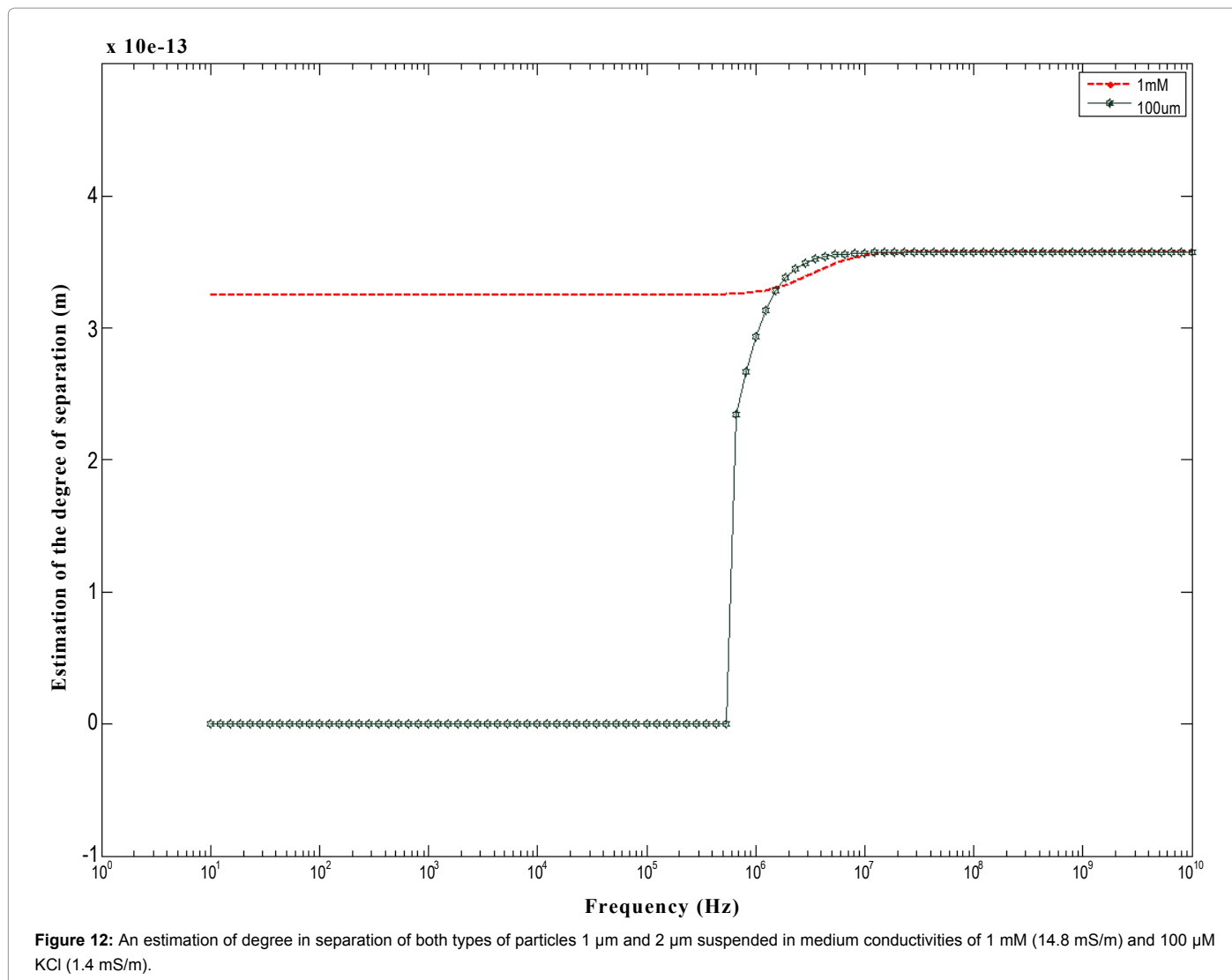


Figure 11: The graph shows the deflection of 2  $\mu\text{m}$  particle from the wall in 1.4 mS/m medium. In this medium the 2  $\mu\text{m}$  particle are experiencing weak positive DEP below 600-700 kHz and thus few particles are leaving the array, therefore in this condition is considered invalid for deflection measurement.



again negative DEP is dominant. It is shown that the 2  $\mu\text{m}$  particles can be deflected farther than the 1  $\mu\text{m}$  particles. The larger particles move towards the other side of the tips of the electrode arrays. This is because ultimately DEP force is only dependent on the size of the particle. It is concluded that as particle size increases, the DEP force exerted on it also increases. Again, due to voltage attenuation at higher frequencies, deflection distance is reduced.

Attenuation of the voltage at higher frequencies is due to the probes used both for electrode signal application and measurements. The waveform generator and the oscilloscope used for these purposes cannot overcome power loss during measurement due to the increase in probe impedance at higher frequencies [59]. The increase in impedance is also caused by the use of higher conductivity mediums where the resistance is higher as compared to the lower conductivity medium.

## Conclusion

This paper shows the successful of the characterization of the angled microelectrode designed and fabricated for the use of particles separation. The experiment performed shows that the separation of particles using the device designed can be achieved 100% when the device pulsed at an intermediate frequency of 1 MHz and at voltage

of 10V [60]. The device is effectively constructed and the experiment conducted has established an important understanding on how mixture of particles of sizes 1  $\mu\text{m}$  and 2  $\mu\text{m}$  react to the changes of applied electrical signal and frequency.

## Acknowledgement

Authors would like to acknowledge Dr. Nicolas G. Green for his valuable and constructive suggestions during the progress and finishing of this work and the facilities provided at Nano Group, School of Electronics and Computer Science, University of Southampton, Highfield, United Kingdom.

## Funds and Grants

This work was conducted at University of Southampton and supported by Ministry of Education Malaysia. It is also supported by GP-IBT/2013/9417600 Putra Grant under research program, Electron Devices and Systems and research group Microelectronic Lab on Chip for Life Sciences and Environment, Department of Electrical and Electronic Engineering, Universiti Putra Malaysia.

## References

1. Yunus NAM, Green NG (2008) Dielectrophoretic Separation of Colloidal Particles using Angled Electrode Arrays. The 12th International Conference on Miniaturized Systems for Chemistry and Life Sciences, San Diego, USA.
2. Pohl HA (1978) Dielectrophoresis: The Behavior of Neutral Matter in Nonuniform Electric Fields. Cambridge University Press Cambridge, UK.

3. Gascoyne PRC, Vykoukal JV (2004) Dielectrophoresis-based Sample Handling in General-Purpose Programmable Diagnostic Instruments. *Proceedings of the IEEE* 92: 22-42.
4. Durán R, Ramirez A, Zehe A (2006) Nano-rotor driven by the electrorotation effect acting on a cylindrical bioparticle. *Proceedings of the 2006 WSEAS International Conference on Mathematical Biology and Ecology*, Miami, Florida.
5. Pethig R (1979) *Dielectric and Electronic Properties of Biological Materials*. John Wiley & Sons.
6. Huang Y, Pethig R (1991) Electrode Design for Negative Dielectrophoresis. *Measurement Science & Technology* 2: 1142-1146.
7. Suehiro J, Pethig R (1998) The Dielectrophoretic Movement and Positioning of a Biological Cell using A Three-Dimensional Grid Electrode System. *Journal of Physics-London-D Applied Physics* 31: 3298-3305.
8. Pethig R, Bressler V, Crumpton CC, Chen Y, Haje LF, et al. (2002) Dielectrophoretic Studies of the Activation of Human T lymphocytes using A Newly Developed Cell Profiling System. *Electrophoresis* 23: 2057-2063.
9. Marx GH, Rousselet J, Pethig R (1997) DEP-FFF: Field-flow Fractionation Using Non-Uniform Electric Fields. *Journal of Liquid Chromatography & Related Technologies* 20: 2857-2872.
10. Marx GH, Pethig R, Rousselet J (1997) The Dielectrophoretic Levitation of Latex Beads, With Reference to Field-flow Fractionation. *Journal of Physics D-Applied Physics* 30: 2470-2477.
11. Pethig R (1984) *Dielectric Properties of Biological Materials: Biophysical and Medical Applications*. *IEEE Transactions on Electrical Insulation* 453-474.
12. Pethig R, Kell DB (1987) The Passive Electrical Properties of Biological Systems: Their Significance in Physiology, Biophysics and Biotechnology. *Phys Med Biol* 32: 933-970.
13. Pethig R (1987) Dielectric Properties of Body Tissues. *Clinical Physics and Physiological Measurement* 8: 5-12.
14. Pethig R, Marx GH (1997) Applications of Dielectrophoresis in Biotechnology. *Trends in Biotechnology* 15: 426-432.
15. Fuhr G, Arnold WM, Hagedorn R, Muller T, Benecke W, et al. (1992) Levitation, Holding, and Rotation of Cells within Traps Made by High-Frequency Fields. *Biochimica Et Biophysica Acta* 1108: 215-223.
16. Muller T, Gerardino A, Schnelle T, Shirley SG, Bordoni F, et al. (1996) Trapping of Micrometre and Sub-micrometre Particles by High-Frequency Electric fields and Hydrodynamic forces. *Journal of Physics D-Applied Physics* 29: 340-349.
17. Muller T, Gradl G, Howitz S, Shirley S, Schnelle T, et al. (1999) A 3-D Microelectrode System for Handling and Caging Single Cells and Particles. *Biosensors & Bioelectronics* 14: 247-256.
18. Schnelle T, Muller T, Fiedler S, Fuhr G (1999) The Influence of Higher Moments on Particle Behaviour in Dielectrophoretic Field Cages. *Journal of Electrostatics* 46: 13-28.
19. Schnelle T, Muller T, Fuhr G (2000) Trapping in AC Octode Field Cages. *Journal of Electrostatics* 50: 17-29.
20. Gimsa J, Marszalek P, Loewe U, Tsong TY (1991) Dielectrophoresis and Electrorotation of Neurospora Slime and Murine Myeloma Cells. *Biophysical Journal* 60: 749-760.
21. Gimsa J, Wachner D (1998) A Unified Resistor-Capacitor Model for Impedance, Dielectrophoresis, Electrorotation, and Induced Transmembrane Potential. *Biophysical Journal* 75: 1107-1116.
22. Gimsa J, Wachner D (1999) A Polarization Model Overcoming the Geometric Restrictions of the Laplace Solution for Spheroidal Cells: Obtaining New Equations for Field-Induced Forces and Transmembrane Potential. *Biophysical Journal* 77: 1316-1326.
23. Gimsa J (2001) A Comprehensive Approach to Electro-orientation, Electrodeformation, Dielectrophoresis, and Electrorotation of Ellipsoidal Particles and Biological Cells. *Bioelectrochemistry* 54: 23-31.
24. Weigl BH, Yager P (1999) Microfluidic Diffusion-based Separation and Detection. *Science* 283: 346.
25. Pohl HA (1951) The Motion and Precipitation of Suspensoids in Divergent Electric Fields. *Journal of Applied Physics* 22: 869.
26. Jones TB (1995) *Electromechanics of Particles*. Cambridge; New York: Cambridge University Press.
27. Markov KZ (2000) *Elementary Micromechanics of Heterogeneous Media. Heterogeneous Media: Micromechanics Modeling Methods and Simulations* 1-162.
28. Atkins PW, Kropf A (1987) The Second Law. *American Journal of Physics* 55: 91.
29. Bockris JOM, Reddy AKN (1973) *Modern Electrochemistry: An Introduction to An Interdisciplinary Area*. Springer Science & Business Media, Plenum.
30. Hamon B (1953) Maxwell-Wagner Loss and Adsorption Currents in Dielectrics. *Australian Journal of Physics* 6: 304-315.
31. Maxwell JC (1892) *A Treatise on Electricity and Magnetism*. Oxford : Clarendon Press.
32. Chen DF, Du H, Li WH (2006) A 3D Paired Microelectrode Array for Accumulation and Separation of Microparticles. *Journal of Micromechanics and Microengineering* 16: 1162-1169.
33. D. Chen and H. Du (2007) A Dielectrophoretic Barrier-based Microsystem for Separation of Microparticles. *Microfluidics and Nanofluidics* 3: 603-610.
34. Chen CX, Zhang YF (2006) Manipulation of single-wall carbon nanotubes into dispersively aligned arrays between metal electrodes. *Journal of Physics D-Applied Physics* 39: 172-176.
35. Kralj JG, Lis MTW, Schmidt MA, Jensen KF (2006) Continuous Dielectrophoretic Size-Based Particle Sorting. *Anal Chem* 78: 5019-5025.
36. Wang L, Flanagan LA, Jeon NL, Monuki E, Lee AP (2007) Dielectrophoresis switching with vertical sidewall electrodes for microfluidic flow cytometry. *Lab on a Chip* 7: 1114-1120.
37. Demierre N, Braschler T, Linderholm P, Seger U, Lintel H, et al. (2007) Characterization and optimization of liquid electrodes for lateral dielectrophoresis. *Lab on a Chip* 7: 355-365.
38. Yunus NAM, Jaafar H, Halin IA, Jasni J (2014) The demand model of electric field strength on microelectrode designed for AC electrokinetic applications. 9th IEEE International Conference on Nano/Micro Engineered and Molecular Systems (NEMS).
39. Yunus NAM, Green NG (2015) Dielectrophoretic Characterization of Colloidal Particles Using Angled Microelectrode Arrays. *Fluid Mechanics and Heat & Mass Transfer (FLUIDSHEAT '15)*, WSEAS2015.
40. Yunus NAM, Green NG (2008) Continuous Separation of Submicron Particles Using Angled Electrode. *Journal of Physics: Conference Series* 142.
41. Li W, Sun J, Liu B, Zhang XZ (2007) Simulation Study of Quadrupole Dielectrophoretic Trapping. 4th WSEAS International Conference on Fluid Mechanics 1-7.
42. Wang F, Tan WB, Zhang Y, Fan X, Wang M (2006) Luminescent nanomaterials for biological labeling. *Nanotechnology* 17: R1.
43. Green NG, Morgan H (1997) Dielectrophoretic Separation of Nanoparticles. *Journal of Physics D-Applied Physics* 30.
44. McManus GB, Fuhrman JA (1986) Bacterivory in seawater studied with the use of inert fluorescent particles. *Limnology and oceanography* 420-426.
45. Wang YC, Han J (2008) Pre-binding dynamic range and sensitivity enhancement for immuno-sensors using nanofluidic preconcentrator. *Lab Chip* 8: 392-394.
46. Rembaum A, Yen SPS, Dreyer WJ (1979) Preparation of small bio-compatible microspheres. Google Patents.
47. Liu G, Wang J, Wu H, Lin Y (2007) Nanovehicles based bioassay labels. *Electroanalysis* 19: 777-785.
48. Marquette CA, Cretich M, Blum LJ, Chiari M (2007) Protein microarrays enhanced performance using nanobeads arraying and polymer coating. *Talanta* 71: 1312-1318.
49. Swanton EM, Curby WA, Lind HE (1962) Experiences with the Coulter counter in bacteriology. *Applied and Environmental Microbiology* 10: 480.
50. Holmes D, Morgan H (2010) Single cell impedance cytometry for identification and counting of CD4 T-cells in human blood using impedance labels. *Analytical Chemistry* 82: 1455-1461.

51. Schroeder F, Kinden DA (1983) Measurement of phagocytosis using fluorescent latex beads. *Journal of Biochemical and Biophysical Methods* 15-27.
52. Lehmann AK, Sornes S, Halstensen A (2000) Phagocytosis: measurement by flow cytometry. *Journal of immunological methods* 243: 229-242.
53. Thomas RSW, Mitchell PD, Oreffo ROC, Morgan H (2010) Trapping single human osteoblast-like cells from a heterogeneous population using a dielectrophoretic microfluidic device. *Biomicrofluidics* 4: 02-15.
54. Pethig R (2010) Preface to Special Topic: Dielectrophoresis. *Biomicrofluidics* 4: 022701.
55. Sun T, Tsuda S, Zauner KP, Morgan H (2010) On-chip electrical impedance tomography for imaging biological cells. *Biosensors and Bioelectronics* 25: 1109-1115.
56. Slopek RP, Gilchrist JF (2010) Self-assembly of wires in acrylate monomer via nanoparticle dielectrophoresis. *Journal of Physics D: Applied Physics* 43: 045402.
57. Gunda NSK, Mitra SK (2010) Modeling of dielectrophoretic transport of myoglobin molecules in microchannels. *Biomicrofluidics* 4: 014105.
58. Yunus NAM, Green NG (2008) Continuous separation of submicron particles using angled electrodes. *Journal of Physics: Conference Series* 142: 012068
59. Wei TS, Sulaiman N, Kamsani NA, Yunus NAM (2014) Dual control Direct Digital Synthesizer (DCDDS) for electronic testing and experimental work. 4th International Conference on Engineering Technology and Technopreneuship (ICE2T), Malaysia.
60. Yunus NAM, Nili H, Green NG (2013) Continuous Separation of Colloidal Particles Using Dielectrophoresis. *Electrophoresis* 34: 969-978.